Supporting information

Mesocrystalline Effect in $NiTiO_3/TiO_2$ Nanocomposite for Enhanced Capacity of Lithium-ion Battery Anode

Xing Wang[a], Weijie Cheng[b], Jiaqiao Hu[b], Ying Su[b], Xingang Kong[b], Shinobi Uemura[a], Takafumi Kusunose[a], Qi Feng[a*]

[a] Department of Advanced Materials Science, Faculty of Engineering and Design, Kagawa University, 2217-20 Hayashi-cho, Takamatsu-shi, 761-0396, Japan

[b] School of Materials Science and Engineering, Shaanxi University of Science and Technology, Weiyang, Xi'an, Shaanxi, 710021, PR China

* Corresponding author. Department of Advanced Materials Science, Faculty of Engineering and Design, Kagawa University, 2217-20 Hayashi-cho, Takamatsu-shi, 761-0396, Japan

E-mail *address*: feng.qi@kagawa-u.ac.jp

Synthesis of L-$NiTiO_3/TiO_2$ nanocomposites from Ni-HTO ion exchanged products

The Ni^{2+}-exchanged HTO (Ni-HTO) sample was obtained by treating 0.5 g of HTO in a 0.5 mol/L Ni $(CH_3COO)_2$ solution (100 mL) under stirring conditions for 12 h. The Ni-HTO sample was heated in air atmosphere at 600 ^oC for 3 h to obtain a

$NiTiO_3/TiO_2$ nanocomposite sample (L-$NiTiO_3/TiO_2$) with low $NiTiO_3$ content.

Table S1 Molar ratios of Ni/Ti in Ni-HTO, Ni-H_2O_2-HTO, Ni-HTO-ns and Ni-H_2O_2-HTO-ns.

Samples	Ni/Ti (At%)
Ni-HTO	0.046
Ni-H_2O_2-HTO	0.347
Ni-HTO-ns	0.480
Ni-H_2O_2-HTO-ns	0.734

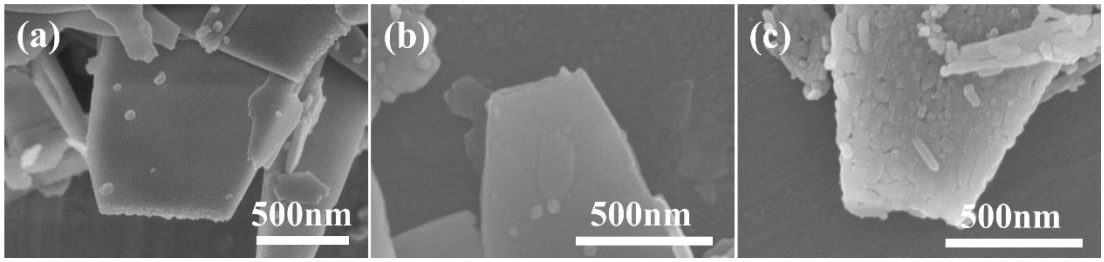

Fig. S1 FE-SEM images of (a) H_2O_2-HTO, (b)Ni-HTO and (c) products after heated Ni-HTO at 600 ℃.

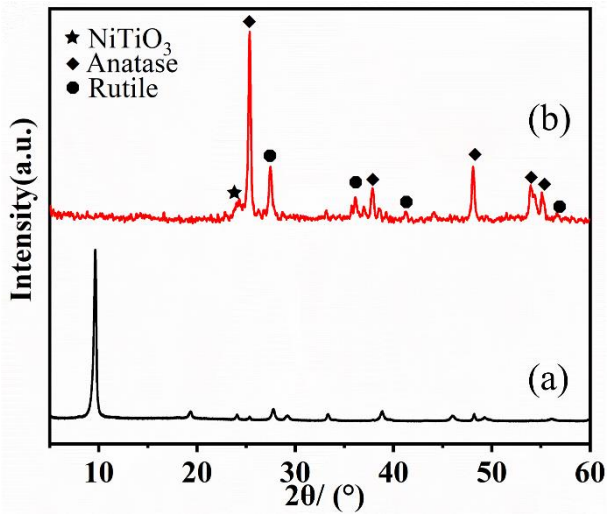

Fig. S2 XRD patterns of (a) Ni-HTO and (b) product after heat-treatment of Ni-HTO at 600 ℃.

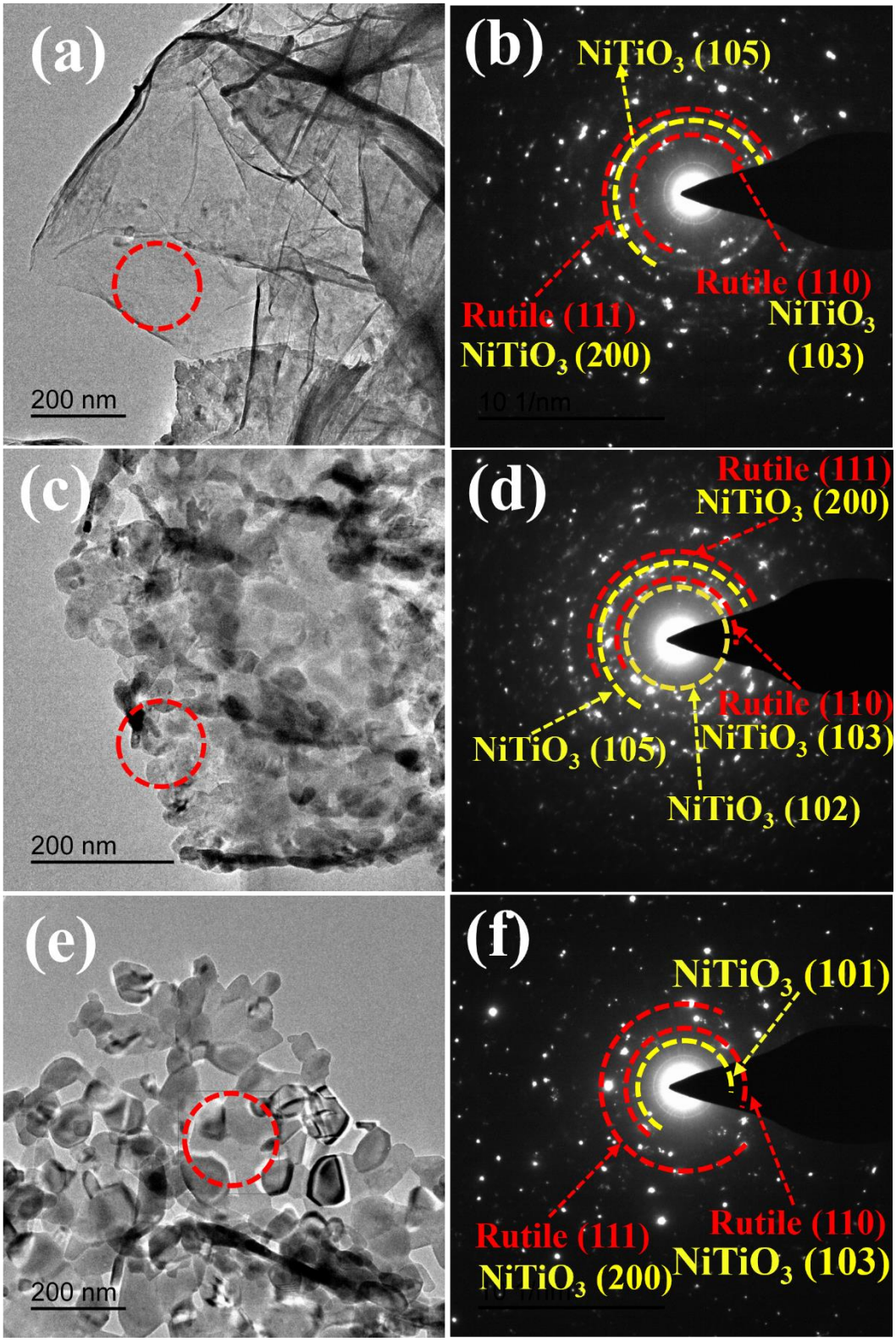

Fig.S3 TEM images and SAED patterns of (a, b) Ni-H_2O_2-HTO-ns-500, (c, d) Ni-H_2O_2-HTO-ns-600, (e, f) Ni-H_2O_2-HTO-ns-700

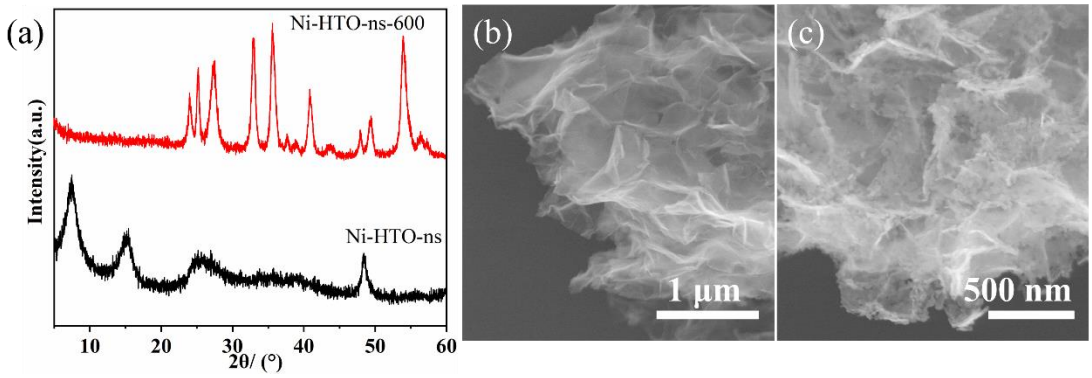

Fig. S4 XRD patterns of (a) Ni-HTO-ns and its heat-treated product at 600°C, FE-SEM images of (b) Ni-HTO-ns and (c) its heat-treated product at 600°C.

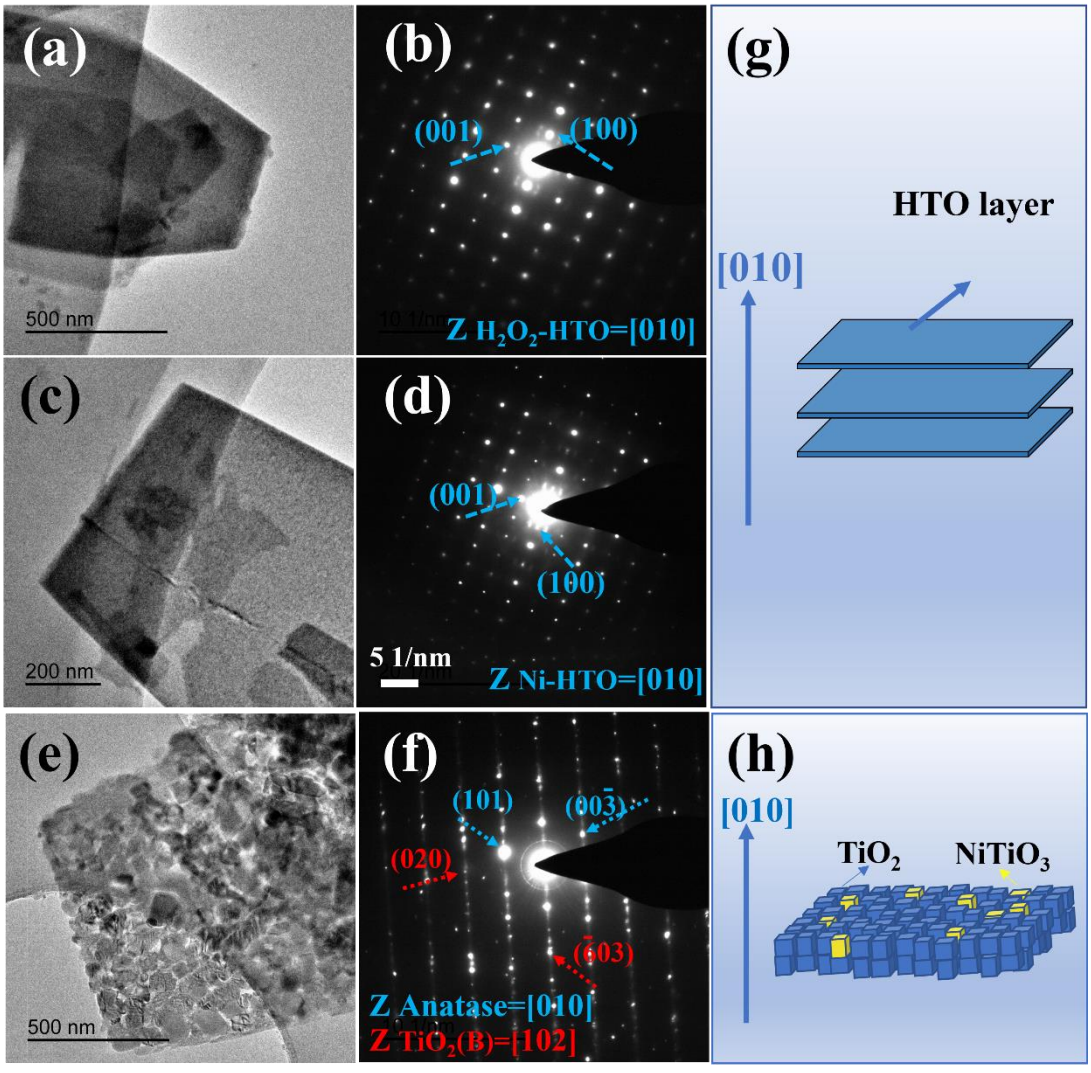

Fig. S5 TEM images and SAED patterns of (a, b) H_2O_2-HTO, (c, d) Ni-HTO, (e, f) Ni-HTO-600, and (g, h) corresponding layered structures.

Ni-HTO has a platelike particle morphology and shows a SAED pattern similar to

HTO and H_2O_2-HTO. In the SAED pattern (Fig. S5(b)), one set of single crystalline diffraction spots with *d*-values of 3.73 nm and 2.96 nm were observed, which correspond to (100) and (001) planes of HTO, respectively, suggesting that [010]-crystal-axis of H_2O_2-HTO phase is vertical to the basal plane of the platelike particle, as shown in Fig. S4 (g).

The TEM result indicated that the Ni-HTO-600 also possesses the platelike particle morphology constructed from nanocrystals with size of about 50 nm (Fig. S5(e)). The SAED patterns display two sets of single-crystal-like diffraction spots. One set with *d*-values of 0.352 and 0.317 nm can be attributed to (101) and $(00\bar{3})$ planes of anatase, respectively (Fig. S5(f)). And another set corresponds to (020) and $(\bar{6}03)$ planes of TiO_2(B), consistent with the previous study.[1] The SAED result suggests all the anatase nanocrystals have the same orientation to [010]-crystal-axis and all TiO_2(B) nanocrystals have the same orientation to [102]-crystal-axis, namely it is a mesocrystalline nanocomposite. The diffraction spots of $NiTiO_3$ were not observed due to it low content in the nanocomposite.

Reference

1. D. Hu, W. Zhang, Y. Tanaka, N. Kusunose, Y. Peng and Q. Feng, *Cryst. Growth Des.*, 2015, **15**, 1214-1225.

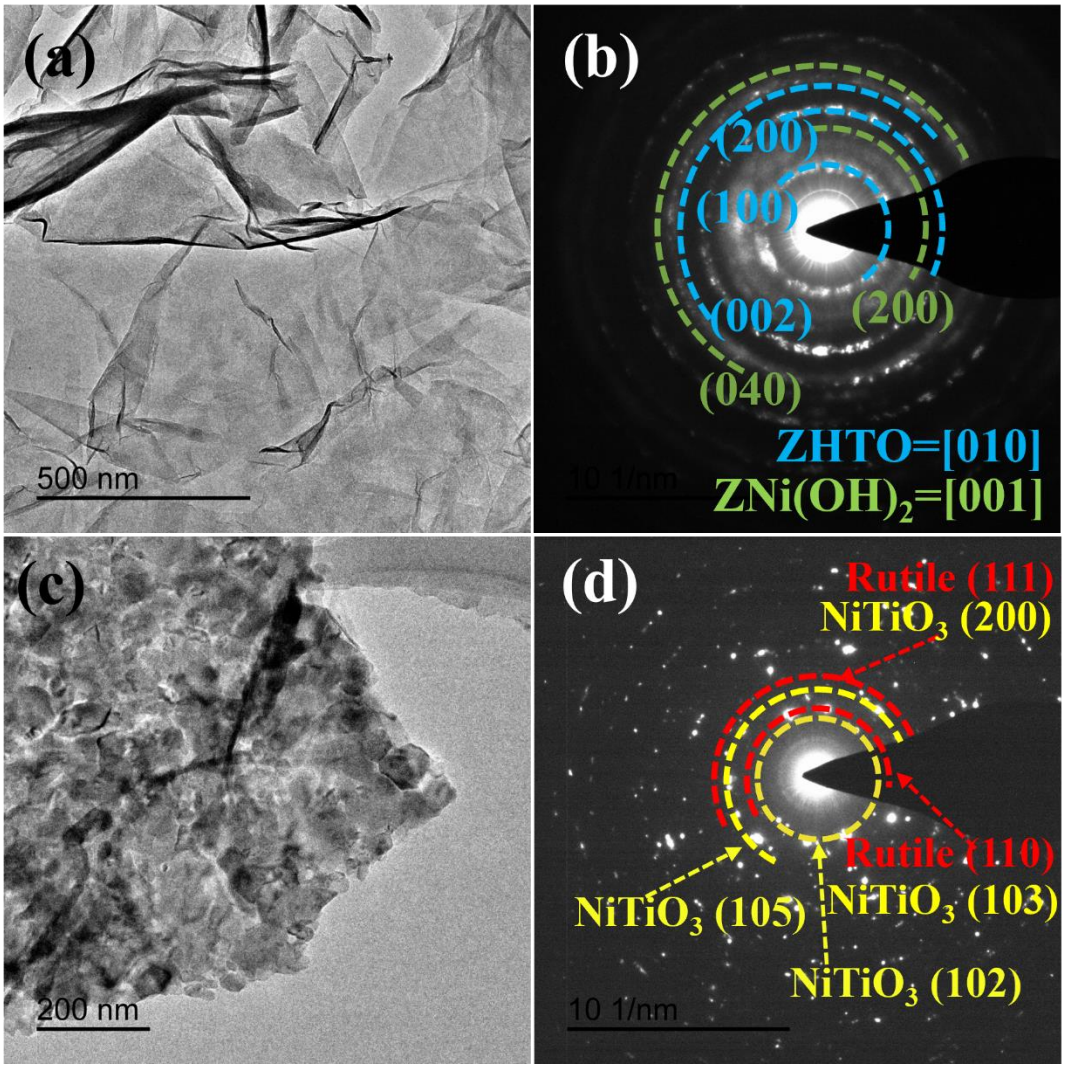

Fig. S6 TEM images and SAED patterns of (a, b) Ni-HTO-ns, (c, d) Ni-HTO-ns-600.

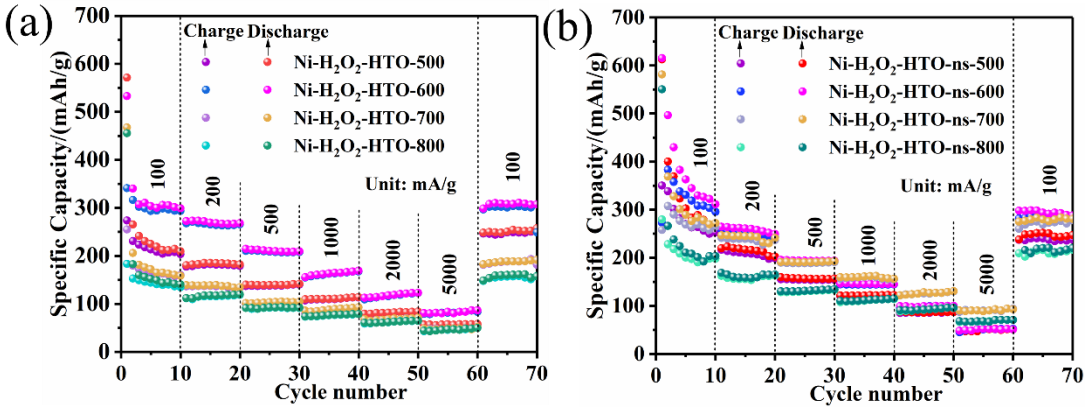

Fig. S7 Rate capabilities of (a) mesocrystalline $NiTiO_3/TiO_2$ nanocomposites and (b) polycrystalline $NiTiO_3/TiO_2$ nanocomposites obtained by heat-treatment of Ni-H_2O_2-HTO and Ni-H_2O_2-HTO-ns at 500, 600, 700 and 800 °C, respectively.

Table S2 Calculated parameters from Nyquist plots and equivalent circuit for Ni-HTO-ns-600 and Ni-H_2O_2-HTO-600 electrodes after 100th cycle at a current density of 100 mA/g in the frequency range of 100kHz to 0.01 Hz.

Samples	Re (Ω)	Rs (Ω)	Rct (Ω)	σ (Ω cm^2 s$^{-0.5}$)	D_{Li+} (cm^2 S^{-1})
Ni-HTO-ns-600	6.9	75.8	473.7	1418	1.05x10^{-17}
Ni-H_2O_2-HTO-600	5.9	58.2	305.3	956	2.31x10^{-17}

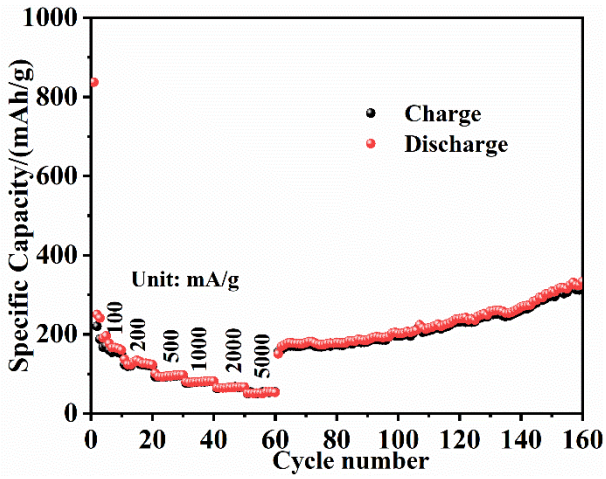

Fig. S8 Rate capabilities and cycle performance at 100 mA/g for pure $NiTiO_3$ obtained by solid-state reaction.

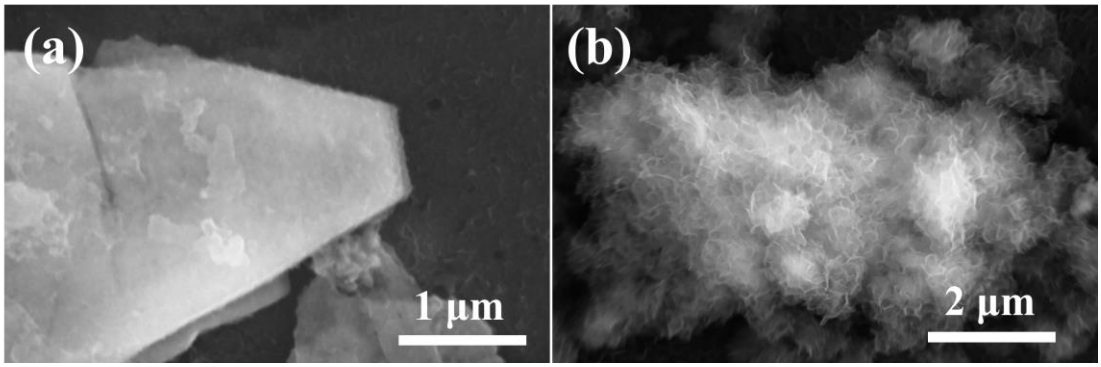

Fig. S9 *Ex-situ* SEM images of (a) Ni-H_2O_2-HTO-600 (b) Ni-H_2O_2-HTO-ns-600 after 100 cycles at 100 mA/g.

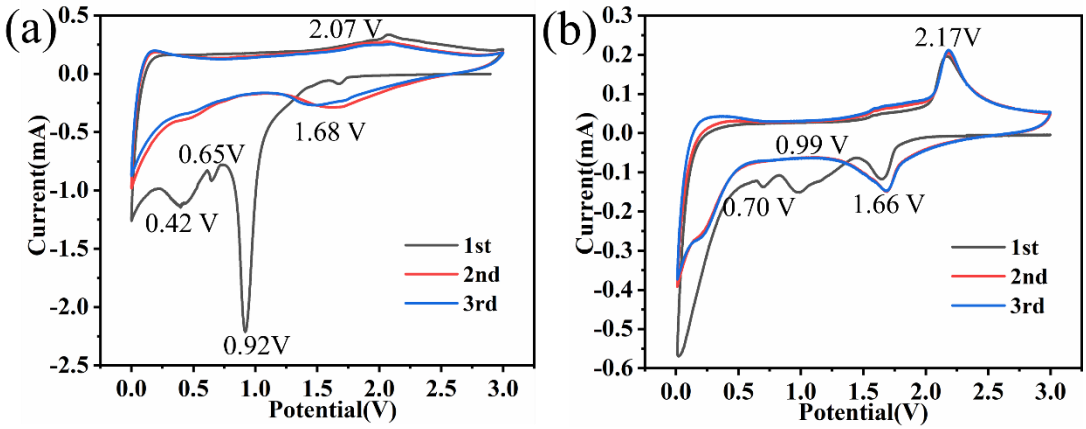

Fig. S10 Cyclic voltammetry (CV) curves of (a) Ni-H_2O_2-HTO-ns-600 and (b) Ni-H_2O_2-HTO-600 at scan rate of 0.1mV/s.

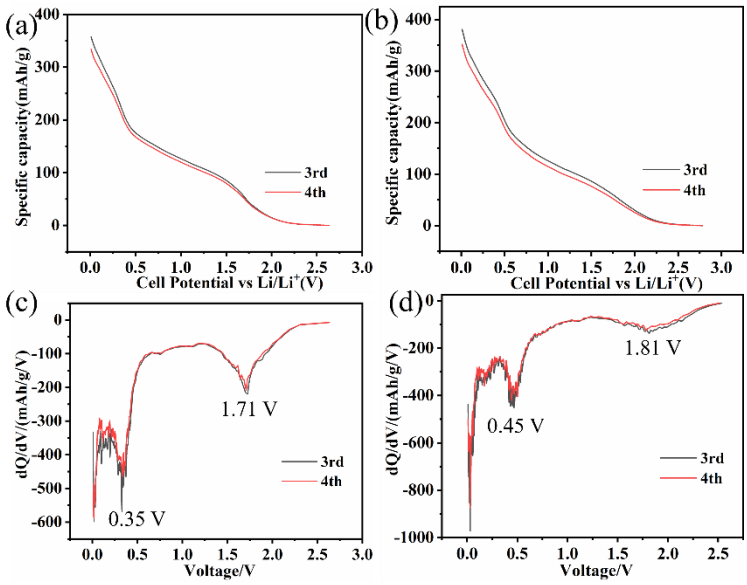

Fig. S11 Discharge profiles at a current density of 100 mA/g for (a) Ni-H_2O_2-HTO-600 and (b) Ni-H_2O_2-HTO-ns-600; dQ/dV discharge curves for (c) Ni-H_2O_2-HTO-600 and (d) Ni-H_2O_2-HTO-ns-600 obtained from their discharge profiles.